Mapping the frontier electronic structures of triphenylamine basedorganic dyes at TiO2 interfaces

Maria Hahlin, M Odelius, Martin Magnuson, Erik Johansson, S Plogmaker, D Hagberg, L Sun, H Siegbahn and H Rensmo

Original Publication:

Maria Hahlin, M Odelius, Martin Magnuson, Erik Johansson, S Plogmaker, D Hagberg, L Sun, H Siegbahn and H Rensmo, Mapping the frontier electronic structures of triphenylamine basedorganic dyes at TiO2 interfaces, 2011, Physical Chemistry, Chemical Physics - PCCP, (13), 8, 3534-3546.
http://dx.doi.org/10.1039/c0cp01491e

Mapping the Frontier Electronic Structures of triphenylaneline based Organic Dye/TiO_2 Interfaces

Maria Hahlin[a], Michael Odelius[b], Martin Magnusson[c], Erik M.J. Johansson[d], Stefan Plogmaker[a], Daniel P Hagberg[e], Licheng Sun[e], Hans Siegbahn[a], Håkan Rensmo[a]

[a] Department of Physics and Astronomy, Uppsala University, Box 516, SE-751 20 Uppsala, Sweden
[b] Department of Physics, Stockholm University, AlbaNova University Center, 106 91 Stockholm, Sweden,
[c]
[d] Department of Physical and Analytical chemistry, Uppsala University, Box 259, 751 05 Uppsala, Sweden
[e] Center of Molecular Devices, Royal Institute of Technology, Chemical Science and Engineering, Organic Chemistry, 100 44 Stockholm, Sweden

Abstract

The electronic and molecular properties of dye molecules 3-(5-(4-(diphenyl amino) styryl) thiophen-2-yl)-2-cyanoacrylic acid (D5L2A1), 3-(5-bis(4-(methoxy phenylamino)styryl) thiophen-2-yl)-2-cyanoacrylic acid (D9L2A1), (D5A1), and (L2A1) are investigated using photoelectron spectroscopy(PES), X-ray absorption spectroscopy(XAS), X-ray emission spectroscopy(XES) and resonant photoelectron spectroscopy (RPES), and the results are compared to theoretical calculations. The combination of experiment and theory on the series of dyes allows for a decomposition of the electronic structure into functional groups and the mutual influence as these building blocks are joint together.

1 Introduction

Dye-sensitized solar cells (DSC) has received wide spread interest as a promising alternative to conventional solar cells.[1–3] In the DSC, the dye adsorbs light through a charge-separating excitation. The dyes are adsorbed on a nanostructured TiO_2 network and the light adsorption is followed by a fast injection of the excited electron into the conduction band of the TiO_2 network and subsequently transported to the back contact. The oxidized dye is reduced by the transfer of electrons from a redox mediator.

The most efficient DSCs, with efficiencies reaching over 10%, uses metal complexes, such as ruthenium polypyridines (N3, N719 and black dye), as light harvesting material, and a liquid based electrolyte containing the redox couple I^-/I_3^- as redox mediator.[1–3] In resent years there has been an increasing interest in organic dyes as light harvesting material.[4–19] Specifically the organic sensitizers compete with the more traditional dyes in the thin solid solar cells where high extinction coefficients of the dyes are needed for efficient light harvesting. The relatively easy synthetic routes of organic dye makes them easy to modify with respect to position of the energy levels important for the DSC energy conversion.

The dyes in this investigation are constructed using three units, the triphenylaneline moiety (referrred to as the D5 unit and with the methoxy units as the D9 unit), a thiophene moiety (referred to as the L2 unit), and the cyanoacrylic acid moiety (referred to as the A1 unit). A goal of this investigation is to understanding the contribution of each unit to the total electronic composition and in doing so to contribute to further understanding in the field of dye design.

The efficiency of the solar cell is largely dependent on the molecular properties of the interfacial region between the DSC materials. Therefore, information about the interfaces is of great importance in understanding the function of the solar cell. In the present study we use photoelectron spectroscopy (PES), resonant photoelectron spectroscopy (RPES), X-ray emission spectroscopy (XES), and X-ray absorption spectroscopy (XAS) in combination with theoretical calculations to compare in detail the outermost electronic structure of the organic dyes D9L2A1, D5L2A1, D5A1, and L2A1, see figure 1. PES, XES, and RPES are used to probe the occupied electronic structure and XAS is used to probe the unoccupied orbitals. RPES also allows us to relate information in the occupied and unoccupied levels. All these techniques taken together gives a de-

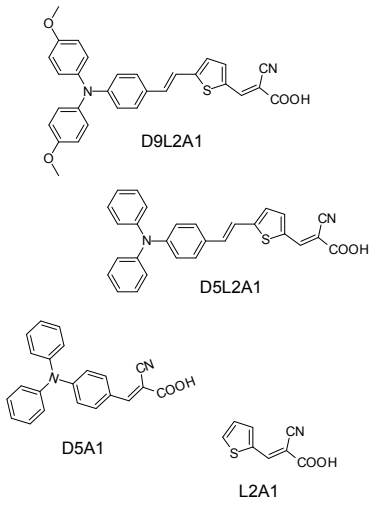

Figure 1: Molecular structure of D9L2A1, D5L2A1, D5A1, and L2*A1.

tailed characterization of the energy matching at the dye-sensitized TiO_2 interfaces.

2 Experimental

2.1 Sample preparation

The synthesis procedure of the D9L2A1, D5L2A1, D5A1, and L2A1 dyes as well as the preparation of TiO_2 colloidal solution are described elsewhere 10,28,30 and [ref TiO_2 paste]. The nanostructured dye-sensitized electrodes is prepared as follows. The colloidal TiO_2 solution is first diluted with ethanol (1:1) in order to produce a thin nanostructured TiO_2 film. The TiO_2 solution is thereafter spread out onto conducting SnO2:F glass pieces. The electrodes are heated to 450°C for 30 minutes. This produces a 1-2 μm thick nanoporous TiO_2 film. The electrodes is then allowed to cool and is immersed into the dye solutions, 1 mM D9L2A1, 1 mM D5L2A1, 1 mM D5A1, 1 mM L2A1 all solved in acetonitrile, for 12 h. The samples are finally rinsed in acetonitrile before dried in air and put in the PES analyzing chamber within ten minutes.

The D5A1, D5L2A1, and D9L2A1 powder sample are prepared by smearing out respective powder onto a F:SnO2 substrate. The formation of a complete multilayer is confirmed from the substantial decrease in the PES Sn signals.

2.2 Measurements

The PES, RPES and XAS measurements are performed using synchrotron radiation at BL I411 at the Swedish national laboratory MAX-lab in Lund. The electron take off angle is 70° and the electron take off direction is collinear with the e-vector of the incident photon beam. N1s XAS spectra are recorded by detection of secondary electrons in partial yield mode and are intensity normalized versus the number of insident photons. The PES spectra are energy calibrated by setting the Ti2p substrate signal to 458.56 eV and the N1s XAS spectra are energy calibrated through measurement of the Ti3p peak using first and second order light. The powder samples are energy calibrated by putting the peak with lowest binding energy at the same position as in the dye-sensitized sample.

The XES measurements were performed at BLI311 at the Swedish national laboratory MAX-lab in Lund.

3 Theory

Density functional (DFT) calculations with gradient-corrected exchange and correlation functionals were performed to study the electronic structure of the isolated molecules depicted in figure 1 and in addition also on the isolated subunits D5,L2 and A1. Geometry optimization, photo-emission and x-ray spectrum calculations were done using the StoBe-deMon code [20] with pure density functionals [21,22] and double-zeta valence basis sets including polarization functions. [23] The time-dependent DFT (TDDFT) calculations of the valence excitations which were performed with the Gaussian 03 program [24] employing the B3LYP hybrid functional [21,25] and triple-zeta valence basis sets including polarization functions [26] to link the information from experiments to the photo-excitation occurring in the solar-cell. To ensure a localization of the core-hole in the case of core-excitations, all other atoms of the same element, as the target of the core-excitation, were described by effective core-potentials. [20,27] The electronic relaxation in the presence of the core-hole was converged using a flexible IGLO basis set [28] on the core-excited atom.

For comparison to the experimental photoemission spectra, we derived the density of states (DOS) from electronic ground state calculations. The total DOS was decomposed into different partial DOS for units in the dyes molecules by projection onto groups of N,C,O and S atoms in a Mulliken analysis. A constant shift of all calculated DOS curves were added for direct comparison to the experimental spectra.

The x-ray emission (XE) spectra were derived from the Kohn-Sham orbitals in an electronic ground state calculation, whereas the x-ray absorption (XA) spectra required calculations with the half core-hole transition potential method[29,30] in combination with a double-basis set procedure in which, after convergence, the basis set was augmented with a large diffuse basis set for an improved description of the Rydberg and continuum states.[31,32] For direct comparison to experiment an additional ΔKohn-Sham correction[33] to the lowest core-excited state was used to shift the entire XA spectrum.

4 Result and Discussion

4.1 Valence electronic structure

Experimental valence spectra: The valence photoelectron spectra for molecular multilayers and surface adsorbed monolayers can be used to experimentally investigate the density and character of the highest occupied energy states. The experimental valence band spectra of both sensitized dye/TiO_2 monolayer as well as multilayer samples of the D9L2A1, D5L2A1, and D5A1 dyes are displayed in figure 2 together with measurements on the bare TiO_2. The measurements were taken using a photon energy of 100 eV. A first observation from a comparison between spectra is the absence of the characteristic TiO_2 substrate O2s peak at a binding energy of approximately 23 eV in the spectra of the dye-sensitized samples. This shows that the contribution from the substrate to the valence band spectra of the dye-sensitized in Figure 2 is negligible.

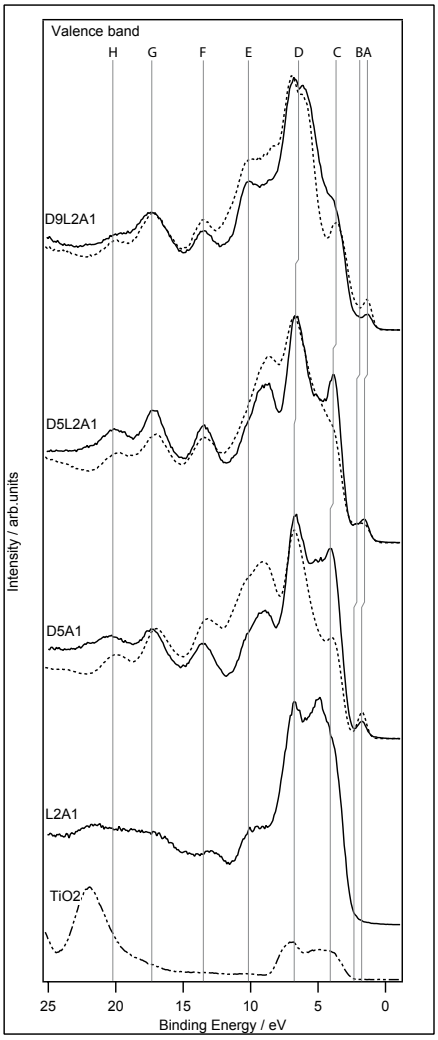

Figure 2: Valenceband spectrum of the L2, D5 and D9 dye-sensitized TiO_2 surface (solid line) and on powder samples (dotted line) measured using photon energy 100 eV.

The valence band spectra of all the monolayer as well as the multilayer samples for D9L2A1, D5L2A1 and D5A1 show large similarities with each other but are clearly different from L2A1. Specifically, the spectral features at a binding energies of 8 eV and higher (E-H) are very similar and this shows that this part of the spectra is largely dominated by the D5/D9 unit. At binding energies lower than 8 eV we observe some spectral changes in the positions referred as A-D. Starting with the two most intense features (C and D) in the region 4-8 eV the spectra for D5L2A1 and D5A1 are similar with one peaks observed at about X eV (D) and one around Y eV (C) although the binding energy position for the latter is slightly higher in D5A1. In comparison the structure for D9L2A1 are clearly different with the D structure split into two and the C structure distributed over a larger energy range. This difference for D9L2A1 is thus attributed to the presence of the methoxy-groups.

The outermost occupied energy levels are vital for electron transfer processes and thus for the function in molecular devices such as solar cells. In figure3 a close up of the experimentally measured HOMO energy levels for D5A1, D5L2A1, D9L2A1 and L2A1 are displayed and it is observed that the outermost occupied energy levels differ both in binding energy position and in shape for the different dyes. The molecules possessing the D5 unit all have a clearly separated spectral features (A and B) located between 1-2 eV binding energy whereas no such peak is observed for L2A1. It is therefore concluded that this structure largely originate from the D5 unit and that it can be spectroscopically observed.

The binding energy position of the outermost peak (A) (HOMO), visible in figure 3 (and summa-

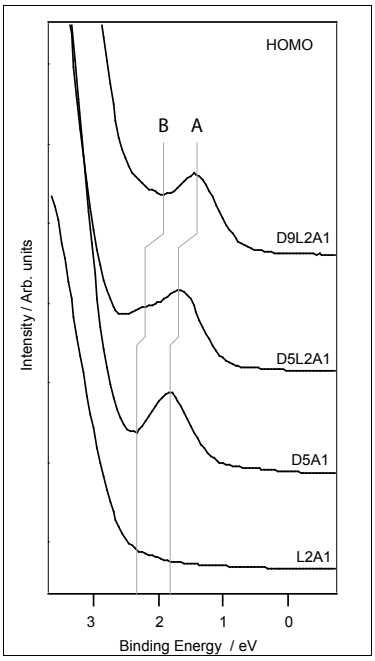

Figure 3: A close up of the outermost region of the valence band, the HOMO energy levels of the L2, D5 and D9 dye-sensitized TiO_2 surface, measured using photon energy 100 eV.

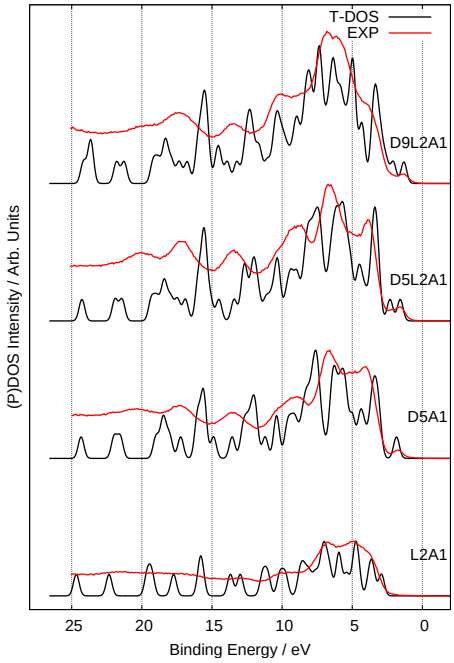

Figure 4: Calculated density of states of D9L2A1, D5L2A1, D5A1 and L2A1. The total DOS(dashed lines) in the calculations are compared to the experimental PES spectra(solid lines). The intensity in the experimental spectra is scaled to fit theory, and the theoretical spectra are shifted by 3.4 eV to align to experiment.

rized in table 1), is highest for the D5A1 followed by the D5L2A1 and D9L2A1. The difference in binding energy is approximately 0.2 eV between the D5A1 and the D5L2A1, showing that the insertion of the L2 unit shift the HOMO level by 0.2 eV towards lower binding energies. The difference between the HOMO of D5L2A1 and D9L2A1 is also approximately 0.2 eV, showing that the HOMO level is further shifted towards lower binding energies by the attachment of methoxy groups on the D5 unit.

The detailed structure of the outermost feature is also different for the three dyes possessing the D5 unit. The D5A1 molecule has a single peak (A) visible at lowest binding energy, whereas for the D5L2A1 molecule clearly two peaks (A and B) are visible in the outermost occupied energy level region, see Figure 3. The experimentally measured binding energy difference between the two lowest HOMO peaks of D5L2A1 is 0.5 eV. In the case of D9L2A1 the outermost peak structure one main peak is observed. However, in comparison with D5A1, the single peak of D5A1 has a more pronounced dip at the higher binding energy side of the peak compared to that of D9L2A1. This finding clearly indicating the presence of some structure at this binding energy region (B) also in the case of D9L2A1 in similarity with that of D5L2A1.

Theoretical DOS and PDOS: Before comparing experimental and theoretical results we will briefly describe the electronic structure in D9L2A1, D5L2A1, D5A1 and L2A1 from a series of density functional (DFT) calculations made on single molecules. The emphasis is to dissect the underlying contributing atomic character and distributions of the valence occupied energy levels in a way that can be used for further understanding of the experimental map obtained from the spectroscopic results.

The theoretically calculated valence band spectra, i.e. the total density of states, tDOS, are displayed in gure 4. In line with the discussion of the experimental spectra the labels A-H are used to describe the spectra and with A referring to the HOMO feature. As expected some similarities are observed for D9L2A1, D5L2A1 and D5A1 while L2A1 are clearly different and the discussion below will mainly focus on the three former.

Starting from the D5L2A1 unit the different features are labeled in Figure 5A. Specifically we observe two peaks (A and B) in the binding energy region 1-3 eV and three pronounced structures (C, D and E) in the binding energy region 3-8 eV. The total density of state, tDOS, are subdivided into partial density of

states, pDOS, for the D5/D9 unit, the L2 unit and the A1 unit in order to further resolve the different contributions. The pDOS for the D5 unit in D5L2A1 largely follows the A-E tDOS structure, while that of A2 and L1 mainly shows similarities with respect to C and B. Specifically this shows that state B and C is distributed over all three units while structure A is mainly centered on the D5 unit. The effect from the methoxy groups can be followed by a comparison between the tDOS for D9L2A1 and D5L2A1. At lower energy a shift in state A and B towards higher energies is observed. For state C the effects are smaller while clear differences are observed in the region of structure D. In this region a new structure appear originating from rather local states centered on the methoxy groups as observed from the methoxy pDOS calculation.

From a comparison between tDOS for D5L2A1 and that obtained for a the D5A1, Figure 5B, the effect from L2 at lower binding energies is mainly a shift of state A and o the appearance of a new state (B) at a binding energy of about 2 eV. Comparing tDOS for D5L2A1 and that obtained for a the L2A1 larger differences are observed and we specifically point out the absence of state A and the pronounced DOS at binding energies between state C and D.

Comparing Experimental Valance spectra and Theoretical DOS: Generally some insight to the complex experimental valence spectrum can be obtained by comparison with theoretical DFT calculations. Such a comparison is shown in figure 4. It is observed that the experimental and theoretical spectra are generally in resonable agreement for all molecules, see Figure 2. All main peaks in the experimental spectra are reproduced in the theoretical spectra showing that the models used are capturing the essential aspects of the dyes although we expect a broadening in the experimental spectra due to variations in geometries and intermolecular interactions. The similarity between theory and experiment motivates the following schematic model of the experimental spectra.

As a starting point we take the electronic structure of the tri-arylamine (a single D5 unit) calculated and shown in Figure 5 and schematically drawn in figure X. The electronic structure may be divided into three main parts, one single level at lower binding energy largely containing the nitrogen lone pair (A), one set of levels shifted a couple of eV containing a mix of the three phenyl centered -orbitals (C) and second set of pi orbitals shifted another few eV (D). Essentially this structure is observed in the experimental spectrum of D5A1 with some contribu-

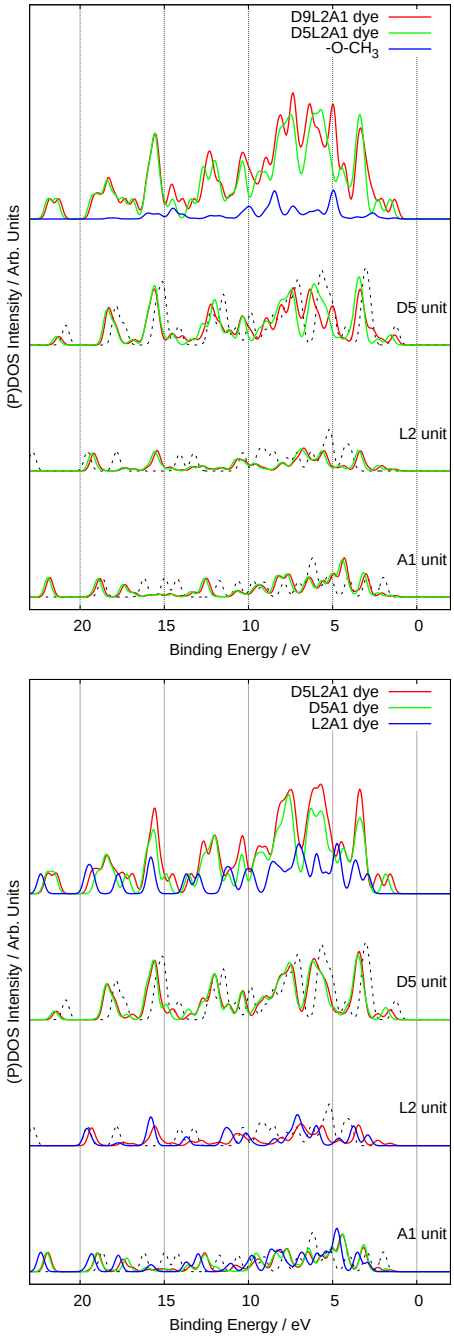

Figure 5: Calculated density of states of D9L2A1, D5L2A1, D5A1 and L2A1. The total DOS at the top is decomposed into partial of the molecular subunits to resolve the electronic structure. The total DOS from separate calculations on the isolated subunits are included in dashed lines.

tion from the NC unit at about 5 eV between C and D and some contribution from the carboxylic group at a position close to structure C. As observed in both the theoretical and experimental results discussed above the incorporation of the tiophene unit L2 in the D5L2A1 molecule gives rise to a new feature (B) at low binding energy. According to the calculations this arise from a mixing of energy levels in D5 with the HOMO levels of the thiophene which splits off part of the manifold structure C to a well-defined level B. (KOLLA MIKAEL). At higher binding energies only small differences are observed in the experimental valence spectra as well as the theoretical DOS when comparing D5L2A1 and D5A1. Finally, we note that the experimentally observed effect from the methoxy groups was followed in the theoretical calculations. The direct effect from the presences of the metoxy group is observed in the broadening of stat D while the shift of HOMO and HOMO-1 is manly an inductive effect since the direct contribution from the methoxy group in these states is very limited (se figure X).

4.2 The unoccupied states N1s XAS spectroscopy

By complementing the photoelectron data on the occupied energy levels with x-ray absorption spectroscopy (XAS) to probe the unoccupied space a complete picture of the electronic structure is obtained. The nitrogen K-edge (N1s) allows us to resolve local projections of the unoccupied states onto the D5 and A1 units. D5 and A1 are natural targets being the functional groups involved in the charge transfer excitation, which governs the electron injection in the solar cells. The experimental N1s-XAS spectra of the D9L2A1, D5L2A1, D5A1, and L2A1 sensitized TiO_2 samples at varying coverage are shown in figure 6, where the number of photoelectrons are plotted versus photon energy. The peaks in the feature below 401 eV in figure 6 are denoted XA, XB and XC. It is observed that all dye-sensitized samples have two sharp resonance features at approximately the same photon energies, 398.4 eV and 399.6 eV. The third peak around 400.5 eV varies with the coverage and is least pronounced for L2A1. Since the L1A1 molecule also possesses these resonances it is concluded that this feature originates from a resonance in the nitrogen atom in the A1 unit.

Furthermore, all N1s-XAS spectra, except for L1A1, contain a broad resonance, denoted XE, at higher photon energies, 405-415 eV, and thus, it is concluded that this resonance structure is mainly generated in the D5/D9 units of all molecules, which has previously been shown for D5L2A1.[?]

At intermediate excitation energies around 402-403 eV, there is a feature, XD, which varies with coverage and possibly splits for the D5A1 dye. Since it does not appear clearly for L1A1, also XD corresponds to states in the triphenylaneline N1s XAS.

In figure 6, the most striking result is the difference in the monolayer and multilayer measurement for the L2A1 molecule. Instead a dominant resonance at 399.6 eV, the N1s-XAS spectrum for the monolayer contains three peak with equal intensity. This is a clear indication of a substantial electronic change in the molecule, which could be caused by strong intermolecules interactions, but which we propose is due to a deprotonation of the L2A1 at the monolayer. Unfortunately, the photoelectron spectrum is not available for L2A1, which would enable us to explore this hypothesis. However, for resolve this issue we can resort to theoreical spectrum simulations. Ideally we would have preferred to also address the small changes in the XC feature at increasing coverage for the triphenylaneline containing dyes with modelling. At the present stage, however, we have too little structural information about these phases to create constraints when building the models to reach a conclusive statement.

The assignments of the experimental N1s-XAS spectra in figure 6 are also confirmed by theoretical calculations presented in figure 7. The strongest peak, XB, is in the calculations assigned to the in-plane anti-bonding C=N orbital. It give a strong signal, since it is a localized state and is not interacting with the conjugated π system. In contrast the XA and XC peaks arise from the out-of-plane anti-bonding C=N orbital which overlaps which contribute to the conjugated π system. In particular the XA level arise from an orbital mixes strongly all the way to the triphenylaneline moiety. In the theoretical calculations of the $N1s_{A1}$ contribution to the XAS spectra the third peak, XC, is clearly visible, located at approximately 400.5 eV, which can only be seen as a shoulder in the dye-sensitized sample.

In the experimental N1s-XAS spectra of D9L2A1, D5L2A1, and D5A1 the fourth peak structure, XD, located at around 402.5 eV, is observed. In this region the theoretical calculations indicates that both the N_{A1} and the N_{D5} contributes approximately equally in intensity. Due to the fact that the position of the experimental peak is more similar to the position of the D5/D9 contribution and also that the XAS spectra above 401 eV has more similarities with the D5/D9 partial contribution we believe that this structure at 402.5 eV is dominated by the resonance in the D5/D9 unit, although no definite assignment of this

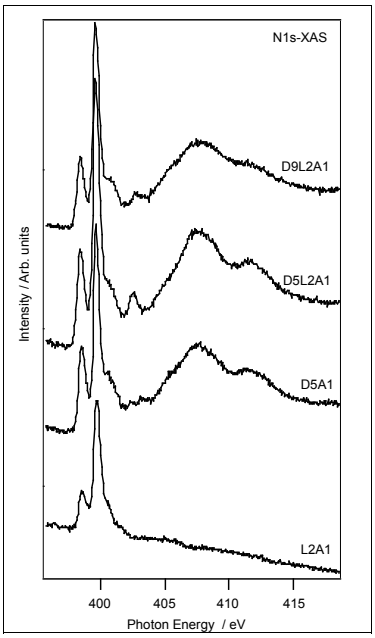

Figure 6: N1s-XAS spectrum of the L2, D5 and D9 dye-sensitized TiO2 surface together with the N1s-XAS spectrum of the multilayered D5 and D9 sample.

resonance is made. The photon energies at which the N1s-XAS resonances in figure 6 occurs are summarized in table 1.

The assignment of the XD peak at 402-404 eV in figure 6 is not possible from the calculations alone. In this region, there are contributions from both the nitrogen atoms, and we can only speculate about which experimental peak corresponds to which orbital. We do notice a correspondnce between how the XD peak is smear as the ether groups added in the D9L2A1 group and the splitting of the triphenylaneline state when going from D5L2A1 to D9L2A1. Nu r Breddade NEXAFS LIKA!!! Jag nr inte energidetaljerna i grafen. As noted in a previous publication, states in the triphenylaneline unit gives rise to the XE peak. **?**

???????????? Rakningar p deprotonated L2A1 haller p.....

However, the electronic structure around the cyano group of the L2A1 molecule is strongly influenced by intermolecular interactions ???or deprotonation??? ??????????

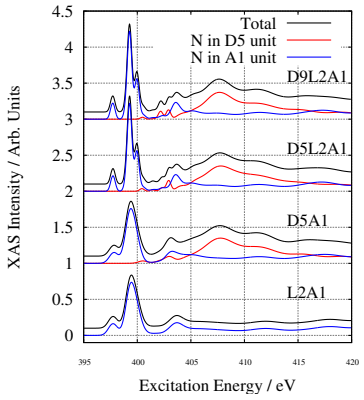

Figure 7: Theoretically calculated N1s-XAS spectra for the dyes in figure 1.

4.3 Experimental map of molecular orbital composition

4.3.1 Resonant and non-resonant XES the nitrogen K-edge

The decay processes from states formed from single photon x-ray excitation or x-ray ionization can be used to experimentally map the pDOS for a molecule with elemental and site specificity. In non-resonant X-ray emission (XES) obtained from a core ionized state (i.e. N1s, in the measurements presented here) the spectrum is described as an emission in a dipole transition between the core ionized and valence ionized state. The local nature of the core hole makes the technique element specific, largely probing the pDOS for a specific element (i.e. N2p). In resonant XES (or resonant inelastic X-ray scattering, RIXS) the incoming photon energy can be selected to match a particular site sensitive absorption energy (e.g. N2p in the NC group). In this case the emission is not just element specific but will reflect the pDOS projected onto a specific atomic site.

The N1s XES spectra for D5 and D9 sensitized TiO2 samples are displayed in figure 6. In order to relate the XES measurements to the experimental DOS as obtained from PES a procedure of positioning the position of the HOMO energy in the XES spectrum by subtracting the energy HOMO-LUMO gap (obtained from the combined PES and XAS measurements, table X) was used. Starting with the non-resonant XES spectra we observe a main structure with emission energy of about 392 eV for both D5L2A1 and D9L2A1. At energies up to 397 eV some structures in the emission is observed while at higher energies no emission is observed. Referencing these measurements to the indicated HOMO energy

Table 1: The binding energies of the N1s

Peak	D9L2A1	D5L2A1	D5A1	L2A1
$N1s_{D5}$	399.60	399.75	399.84	-
$N1s_{A1}$	398.51	398.51	398.89	399.10
$N1s\text{-}XAS^{1st}_{(A1)}$	398.4	398.4	398.5	398.5
$N1s\text{-}XAS^{2nd}_{(A1)}$	399.6	399.6	399.6	399.7
$N1s\text{-}XAS^{3rd}_{(A1)}$ *	400.5	400.5	400.5	400.5
$N1s\text{-}XAS^{4th}_{(D5)}$	402.7	402.5	402.3, 403.1	-
$LUMO^{1st}_{(A1)}$	0.11	0.11	0.34	0.6
$LUMO^{2nd}_{(A1)}$	-1.1	-1.1	-0.76	-0.6
$LUMO^{3rd}_{(A1)}$	-2.0	-2.0	-1.66	-1.4
$LUMO^{4th}_{(D5)}$	-3.1	-2.8	-2.4, 3.2	-
HOMO	1.41	1.66	1.85	-
$\Delta\ E_B^{HOMO-LUMO}$	1.3	1.55	1.51	-

level the experiment indicate that most of the N2p pDOS is positioned 5 eV below the HOMO energy but with some contribution distributed all the way to the HOMO energy level.

Resonant XES spectra are also shown in the figure X. At the bottom the spectra measured with an incoming X-ray energy of 399.15 (KOLLA med XES XAS som ni mtte) eV is shown. For both D5L2A1 and D9L2A1 molecules this energy largely matches the energies of the second XAS resonances having mainly NC character. Both resonant XES spectra are very similar and have a main peak at 391.7 eV indicating that the N2p DOS from the NC group largely appear about 5.3 eV above the HOMO energy. Interestingly both spectra also show a small but clear structure at 396 eV while no clear structures are observed at higher energies. Referencing this to the HOMO energy the results indicate that HOMO (A) has a character not distributed over the NC group but that some such contribution is noticeable in HOMO-1 (B). This is in line with the theoretical results and thus further support the structures displayed in scheme 1.

In figure X also the resonant spectra measured with an incoming energy of 402.05 is shown. For both D5L2A1 and D9L2A1 molecules this energy largely matches the energies of the forth XAS resonances having mainly TAA character. Generally both spectra are rather similar although the shoulder at higher energies is slightly more pronounced in D5L2A1 compared to D9L2A1. Comparing these spectra to those measured at 399.15 the main difference is the intensity at around 397 eV. Since this energy coincide with the position of HOMO energy this strongly indicate the contribution from TAA nitrogen in HOMO (A). Specifically this may be attributed to the mixing of the TAA nitrogen lone pair to the HOMO level and agin support the scheme 1.

4.3.2 Resonant PES

Resonant photoemission spectroscopy (RPES) implies photoemission spectroscopy using a photon energy that coincides (resonance) with the excitation energy of a core orbital to an unoccupied orbital in the system (e.g. energies in the N1s-XAS spectrum), Scheme 1. The excited states formed from the x-ray absorption process primarily decay in an Auger type process leading to electron emission. In analyzing the various features it is useful to classify the RPES transitions into spectator and participator processes. The former imply that the decay occurs without direct involvement of the resonantly excited electron, leading to final states having two holes among the valence orbitals in addition to the excited electron and a signal that is constant in kinetic energy. The participator decay, on the other hand, implies that the resonantly excited electron participates in the decay of the core hole to the final state with an electron in the continuum. Since the final state in the resonant participator decay is the same as in nonresonant photoemission, the participator decay signal is constant in binding energy. Morover, when scanning the photon energies over the N1s XAS resonance energies one thus expect large increas in crossection for states that have similar character as the XAS resonance.

A contour plot of the experimental valence spectra for D9L2A1, D5L2A1, D5A1 and L2A1 adsorbed at TiO2 and taken at the photon energies of the N1s XAS resonances is shown in Figure X. Following the photon energy of the strongest XAS structures originating from the NC group (at 399.6 eV for D9L2A1,

D5L2A1 and D5A1 and 399.7 eV for L2A1) we observe a large increase in cross section at a binding energy of about X eV X eV X eV and X eV, respectivelyr which thus indicate participator contributions. Therefore, the increase in intensity indicates that the NC contribution to the valence structure is rather localized to a binding energy sifted about x eV from the outermost valence level. For D9L2A1 and D5L2A1 these experimental results support the findings obtained from XES and thus the position of the NC groups in scheme 1.

OCH S SISTA FIGURERNA HAR BARA STARTAT VET INTE RIKTIGT VAD VI VILL. Interestingly when comparing the so called CIS spectra in Figure X with those of the N1s XAS we note the absence of an increase of the cross section for absorption on the TAA moiety, indicating delocalization of the electron before the core hole decay. This delocalization may involve the TiO2 substrate and thus be a sign of electron injection within the time domain of the core hole.

5 Acknowledgements

The experimental work was supported by the Swedish Research Council (VR), the Göran Gustafsson Foundation, the Carl Trygger Foundation, the Magnus Bergvall foundation, the Knut and Alice Wallenberg foundation, and the Swedish Energy Agency. We thank the staff at MAX-lab for competent and friendly assistance. The theoretical modeling was made possible through generous allocations of computer time at the Swedish National Supercomputer Center(NSC) and Center for Parallel Computing(PDC), Sweden.

References

[1] M. NAZEERUDDIN, A. KAY, I. RODICIO, R. HUMPHRYBAKER, E. MULLER, P. LISKA, N. VLACHOPOULOS and M. GRATZEL, *JOURNAL OF THE AMERICAN CHEMICAL SOCIETY*, 1993, **115**, 6382–6390.

[2] M. Nazeeruddin, P. Pechy, T. Renouard, S. Zakeeruddin, R. Humphry-Baker, P. Comte, P. Liska, L. Cevey, E. Costa, V. Shklover, L. Spiccia, G. Deacon, C. Bignozzi and M. Gratzel, *JOURNAL OF THE AMERICAN CHEMICAL SOCIETY*, 2001, **123**, 1613–1624.

[3] M. Nazeeruddin, F. De Angelis, S. Fantacci, A. Selloni, G. Viscardi, P. Liska, S. Ito, B. Takeru and M. Gratzel, *JOURNAL OF THE AMERICAN CHEMICAL SOCIETY*, 2005, **127**, 16835–16847.

[4] D. P. Hagberg, T. Edvinsson, T. Marinado, G. Boschloo, A. Hagfeldt and L. Sun, *CHEMICAL COMMUNICATIONS*, 2006, 2245–2247.

[5] E. M. J. Johansson, T. Edvinsson, M. Odelius, D. P. Hagberg, L. Sun, A. Hagfeldt, H. Siegbahn and H. Rensmo, *JOURNAL OF PHYSICAL CHEMISTRY C*, 2007, **111**, 8580–8586.

[6] T. Kitamura, M. Ikeda, K. Shigaki, T. Inoue, N. Anderson, X. Ai, T. Lian and S. Yanagida, *CHEMISTRY OF MATERIALS*, 2004, **16**, 1806–1812.

[7] K. Hara, M. Kurashige, Y. Dan-oh, C. Kasada, A. Shinpo, S. Suga, K. Sayama and H. Arakawa, *NEW JOURNAL OF CHEMISTRY*, 2003, **27**, 783–785.

[8] K. Thomas, J. Lin, Y. Hsu and K. Ho, *CHEMICAL COMMUNICATIONS*, 2005, 4098–4100.

[9] K. Sayama, S. Tsukagoshi, T. Mori, K. Hara, Y. Ohga, A. Shinpou, Y. Abe, S. Suga and H. Arakawa, *SOLAR ENERGY MATERIALS AND SOLAR CELLS*, 2003, **80**, 47–71.

[10] M. Velusamy, K. Thomas, J. Lin, Y. Hsu and K. Ho, *ORGANIC LETTERS*, 2005, **7**, 1899–1902.

[11] I. Jung, J. K. Lee, K. H. Song, K. Song, S. O. Kang and J. Ko, *JOURNAL OF ORGANIC CHEMISTRY*, 2007, **72**, 3652–3658.

[12] D. Shi, Y. Cao, N. Pootrakulchote, Z. Yi, M. Xu, S. M. Zakeeruddin, M. Graetzel and P. Wang, *JOURNAL OF PHYSICAL CHEMISTRY C*, 2008, **112**, 17478–17485.

[13] S. Ito, H. Miura, S. Uchida, M. Takata, K. Sumioka, P. Liska, P. Comte, P. Pechy and M. Graetzel, *CHEMICAL COMMUNICATIONS*, 2008, 5194–5196.

[14] M. Xu, S. Wenger, H. Bala, D. Shi, R. Li, Y. Zhou, S. M. Zakeeruddin, M. Graetzel and P. Wang, *JOURNAL OF PHYSICAL CHEMISTRY C*, 2009, **113**, 2966–2973.

[15] H. Qin, S. Wenger, M. Xu, F. Gao, X. Jing, P. Wang, S. M. Zakeeruddin and M. Graetzel, *JOURNAL OF THE AMERICAN CHEMICAL SOCIETY*, 2008, **130**, 9202+.

[16] M. Wang, M. Xu, D. Shi, R. Li, F. Gao, G. Zhang, Z. Yi, R. Humphry-Baker, P. Wang, S. M. Zakeeruddin and M. Graetzel, *ADVANCED MATERIALS*, 2008, **20**, 4460–4463.

[17] L. Schmidt-Mende, U. Bach, R. Humphry-Baker, T. Horiuchi, H. Miura, S. Ito, S. Uchida and M. Gratzel, *ADVANCED MATERIALS*, 2005, **17**, 813+.

[18] K. R. J. Thomas, Y.-C. Hsu, J. T. Lin, K.-M. Lee, K.-C. Ho, C.-H. Lai, Y.-M. Cheng and P.-T. Chou, *CHEMISTRY OF MATERIALS*, 2008, **20**, 1830–1840.

[19] M. Xu, R. Li, N. Pootrakulchote, D. Shi, J. Guo, Z. Yi, S. M. Zakeeruddin, M. Graetzel and P. Wang, *JOURNAL OF PHYSICAL CHEMISTRY C*, 2008, **112**, 19770–19776.

[20] K. Hermann, L. Pettersson, M. Casida, C. Daul, A. Goursot, A. Koester, E. Proynov, A. St-Amant, and D. Salahub, *Contributing authors: V. Carravetta, H. Duarte, C. Friedrich, N. Godbout, J. Guan, C. Jamorski, M. Leboeuf, M. Leetmaa, M. Nyberg, S. Patchkovskii, L. Pedocchi, F. Sim, L. Triguero, and A. Vela, StoBeDeMon version 2.2 (2006)*.

[21] A. D. Becke, *Phys. Rev. A*, 1988, **38**, 3098.

[22] J. P. Perdew, *Phys. Rev. B*, 1986, **34**, 7406.

[23] N. Godbout, D. Salahub, J. Andzelm and E. Wimmer, *Can. J. Chem.*, 1992, **70**, 560.

[24] M. J. Frisch, G. W. Trucks, H. B. Schlegel, G. E. Scuseria, M. A. Robb, J. R. Cheeseman, J. A. Montgomery, Jr., T. Vreven, K. N. Kudin, J. C. Burant, J. M. Millam, S. S. Iyengar, J. Tomasi, V. Barone, B. Mennucci, M. Cossi, G. Scalmani, N. Rega, G. A. Petersson, H. Nakatsuji, M. Hada, M. Ehara, K. Toyota, R. Fukuda, J. Hasegawa, M. Ishida, T. Nakajima, Y. Honda, O. Kitao, H. Nakai, M. Klene, X. Li, J. E. Knox, H. P. Hratchian, J. B. Cross, V. Bakken, C. Adamo, J. Jaramillo, R. Gomperts, R. E. Stratmann, O. Yazyev, A. J. Austin, R. Cammi, C. Pomelli, J. W. Ochterski, P. Y. Ayala, K. Morokuma, G. A. Voth, P. Salvador, J. J. Dannenberg, V. G. Zakrzewski, S. Dapprich, A. D. Daniels, M. C. Strain, O. Farkas, D. K. Malick, A. D. Rabuck, K. Raghavachari, J. B. Foresman, J. V. Ortiz, Q. Cui, A. G. Baboul, S. Clifford, J. Cioslowski, B. B. Stefanov, G. Liu, A. Liashenko, P. Piskorz, I. Komaromi, R. L. Martin, D. J. Fox, T. Keith, M. A. Al-Laham, C. Y. Peng, A. Nanayakkara, M. Challacombe, P. M. W. Gill, B. Johnson, W. Chen, M. W. Wong, C. Gonzalez and J. A. Pople, *Gaussian 03, Revision C.02*, Gaussian, Inc., Wallingford, CT, 2004.

[25] P. J. Stephens, F. J. Devlin, C. F. Chabalowski and M. J. Frisch, *J. Chem. Phys.*, 1994, **98**, 11623.

[26] J. Guan, P. Duffy, J. T. Carter, D. P. Chong, K. C. Casida, M. E. Casida and M. Wrinn, *The Journal of Chemical Physics*, 1993, **98**, 4753–4765.

[27] L. G. M. Pettersson, U. Wahlgren and O. Gropen, *J. Chem. Phys.*, 1987, **86**, 2176.

[28] W. Kutzelnigg, U. Fleischer and S. M., *NMR-Basic Principles and Progress*, Springer Verlag, Heidelberg, 1990.

[29] J. C. Slater, *Adv. Quantum Chem.*, 1972, **6**, 1.

[30] J. C. Slater and K. H. Johnson, *Phys. Rev. B*, 1972, **5**, 844.

[31] H. Ågren, V. Carravetta, O. Vahtras and L. G. M. Pettersson, *Theor. Chem. Acc.*, 1997, **97**, 14.

[32] L. Triguero, L. G. M. Pettersson and H. Ågren, *Phys. Rev. B*, 1998, **58**, 8097.

[33] C. Kolczewski, R. Püttner, O. Plashkevych, H. Ågren, V. Staemmler, M. Martins, G. Snell, A. S. Schlachter, M. Sant'Anna, G. Kaindl and L. G. M. Pettersson, *J. Chem. Phys.*, 2001, **115**, 6426–6437.